Dramatically improved tensile strength of fullerene needle-like crystals

Toshio Konno[1], Takatsugu Wakahara[2], Kun'ichi Miyazawa[3], Kazuhiro Marumoto[1,4*]

[1]*Division of Materials Science, University of Tsukuba, 1-1-1 Tennodai, Tsukuba, Ibaraki 305-8573, Japan*

[2]*National Institute for Materials Science, 1-1 Namiki, Tsukuba, Ibaraki 305-0044, Japan*

[3]*Imaging Section (IMG), Okinawa Institute of Science and Technology Graduate University (OIST), 1919-1 Tancha, Onna-son, Kunigami-gun, Okinawa, 904-0495, Japan*

[4]*Tsukuba Research Center for Interdisciplinary Materials Science (TIMS), University of Tsukuba, 1-1-1 Tennodai, Tsukuba, Ibaraki 305-8571, Japan*

[*]Corresponding author. Tel.: +81-29-853-5117. E-mail address: marumoto@ims.tsukuba.ac.jp

Abstract

Solid solutions of C_{60}-C_{70} fullerene needle-like crystals were synthesized by liquid-liquid interfacial precipitation using toluene and 2-propanol as solvents, which were bent until fracture using focused ion beam scanning electron microscope for the measurements of their mechanical properties. The C_{60}-C_{70} fullerene needle-like crystals were found to show the tensile strength of 58–71 MPa and the fracture toughness of 1.1–1.3 MPa $m^{\frac{1}{2}}$, where the tensile strength is much higher than that of the C_{60} fullerene needle-like crystals and the specific strength is slightly larger than that of alumina. Moreover, it is possible to change the plasticity and fracture toughness of the C_{60}-C_{70} fullerene needle-like crystals by solvent. Thus, the C_{60}-C_{70} fullerene needle-like crystals are suggested to be applied for materials such as electrodes, anchors as brittle materials, and electric feeder lines as ductile materials.

Key Words: Fullerene nanowhisker, Solid solution, Liquid-liquid interfacial precipitation, Tensile strength, Fracture toughness

Introduction

Carbon atoms can be bonded together by covalent binding to form some carbon allotropes such as fullerenes. A C_{60} fullerene, which is truncated icosahedron molecule, was first observed by Kroto et al. [1]. Fullerenes have been well characterized [2] and reported to exhibit low toxicity [3] with a low cost fabrication [4] to be applied in multiple ways.

One species of the fullerene compounds, molecular fullerene needle-like crystals can be dissolved in organic solvents to recover fullerene molecules [5, 6]. The electrical conductivity of the fullerene needle-like crystals is affected by their diameters, exposure to oxygen, and solvents [7–10]. Thus, these crystals show a potential for the application of field-effect transistors, solar cells, fuel cells, and surface enhanced Raman scattering sensors (SERS) [11–15]. As for the mechanical properties, it has been reported that the C_{60} needle-like crystals have a density of 1.73 g cm^{-3} [16] and a Young's moduli ranging from 32 to 54 GPa [17] which decreases with increasing the crystal diameter and depends on the synthesis conditions [18, 19]. Also, the C_{60} needle-like crystals in air have been reported to be underwent brittle fracture during the bending and the buckling [19–21].

Fullerene needle-like crystals can contain two species of fullerene molecules to form a solid solution with solution hardening. Since substitutional solid solutions can be formed from two species of atoms or molecules which are close in size, we use C_{60} and C_{70} molecules in order to obtain a solid solution in this study. C_{60}-C_{70} needle-like crystals consisting of a C_{60} mother phase doped with 11 wt% C_{70} molecules have been analyzed to exhibit the light absorption band of both C_{60} and C_{70} and a Young's modulus of 60–100 GPa even when the crystal diameter exceeds 1000 nm [22, 23]. Although the C_{60}-C_{70} needle-like crystals are expected to be useful with low density, a high Young's modulus, a wide absorption band, and various electrical conductivities, the mechanical properties of such crystals have not yet been clarified. The understanding of the mechanical properties of the C_{60}-C_{70} needle-like crystals is indispensable to their application as

electric feeder lines, electrode materials, and anchor materials. In this paper, C_{60}-C_{70} needle-like crystals with a diameter of 20–40 μm were synthesized using toluene and 2-propanol as solvents. The crystals were fractured by bending using focused ion beam-scanning electron microscopy (FIB-SEM) to determine their tensile strength, fracture toughness, plastic deformation, and inner structure. The C_{60}-C_{70} fullerene needle-like crystals were found to be brittle materials with the tensile strength much higher than that of C_{60} fullerene needle-like crystals and the specific strength larger than that of alumina.

2. Experimental

The C_{60}-C_{70} fullerene needle-like crystals were synthesized by a liquid-liquid interfacial precipitation method [24]. Fullerene powders (C_{60} 99.5% and C_{70} 98+%, both from MTR Ltd.) were dissolved in toluene (JIS special grade; Wako Pure Chemical Industries Ltd.) using an ultrasonic agitator (Iuchi VS-150; As-One Ltd.). The saturated solutions of C_{60} and C_{70} in toluene were respectively filtered using 450-nm pore filters (Whatman 25 mm GD/X; GE Healthcare UK Ltd.) and mixed using an agitator to give a C_{60}-C_{70} solution containing C_{70} with 45 wt% in toluene as the mother solution.

The mother solution (10 mL) was added to a glass bottle (30 mL, No. 6; As-One Ltd.) and held at 15 °C in a water bath. Then, 2-propanol (10 mL) was slowly layered along the inside wall of the bottle to form a liquid–liquid interface. After mixing the solution by shaking 30 times to promote a homogeneous reaction, the bottle was stored at 15 °C for 5 days to grow needle-like crystals. After replacing the supernatant with 2-propanol, filtration (5B-21; Kiriyama Glass Inc.) under reduced pressure and vacuum drying (VO-300; As-One Ltd.) at room temperature for 120 min were conducted to obtain C_{60}-C_{70} fullerene needle-like crystals.

To fracture the C_{60}-C_{70} fullerene needle-like crystals, the crystals were fixed to a silicon substrate by tungsten deposition, cleaved by gallium ion sputtering, and then bent

using a molybdenum probe until fracture, as outlined in Fig. 1. The fracture surfaces were observed using FIB-SEM (NB5000; Hitachi High-Technologies).

3. Results and Discussion

Fig. 2 shows an SEM image of a representative C_{60}-C_{70} fullerene needle-like crystal. The mean length and mean diameter of the C_{60}-C_{70} fullerene needle-like crystals were obtained to be 168±43 μm and 21±7 μm, respectively.

Figs. 3(a) and (b) depict the SEM images of the fracture surfaces of the C_{60}-C_{70} fullerene needle-like crystals. The fracture surfaces were mostly smooth with some porous structures and contained a small amount of particles and fibrous surfaces. The magnified SEM images of the smooth surfaces with porous structure are presented in Figs. 3(c) and (d). Fullerene needle-like crystals with a porous structure have been reported previously [25]. The porous structure was attributed to rapid evaporation of solvent molecules. The smooth fracture surfaces of the C_{60}-C_{70} fullerene needle-like crystals have been considered to result from brittle fracture [26–27] because the smooth fracture surfaces have been observed for C_{60} fullerene needle-like crystals [19–21]. The brittle fracture of fullerene needle-like crystals has been considered to originate from a stress concentration at the end of the cracks composed of continuous pores [28]. The stress distribution around the end of a crack can be evaluated by the stress intensity factor (K) of three-point bending, schematic of which is shown in Fig. 4, using the following equations [29]:

$$K = F(\xi)\,\sigma_{\mathrm{ben}}\,\sqrt{\pi a},\ \xi = \frac{a}{W},\ F(\xi) = \sqrt{\frac{2}{\pi\,\xi}\tan\frac{\pi\,\xi}{2}}\,\frac{0.923+0.199\,\{1-\sin\frac{\pi\,\xi}{2}\}^4}{\cos\frac{\pi\,\xi}{2}}, \quad (1)$$

where σ_{ben} is the bending stress, a is the length of crack on one side, and W is the thickness of bending samples. σ_{ben} can be calculated using the following equations when a cantilever is applied to a load [30]:

$$\sigma_{ben} = \frac{M}{Z},\ Z = \frac{bh^2}{6},\ M = Px, \quad (2)$$

where M is the bending moment, Z is the section modulus of a rectangular cross section, P is the load, b is the length of the cross section perpendicular to P, h is the length of the cross section parallel to P, and x is the distance between the points of the effort and the load. The flexure δ can be expressed using the P as follows [31]:

$$\delta = \frac{Pl^3}{3EI}, I = \frac{bh^3}{12}, \quad (3)$$

where E is the Young's modulus, I is the second moment of the area on a rectangular cross section, and l is the distance between the points of effort and fulcrum. Eq. (4) is derived from Eqs. (2) and (3):

$$\sigma_{ben} = \frac{3hx\delta E}{2l^3}. \quad (4)$$

According to Figs. 5 (b) and (c), the parameters h = 6.5 μm, l = 46 μm and x = 18 μm or h = 2.1 μm, l = 46 μm and x = 20 μm were obtained for the 1st or 2nd C_{60}-C_{70} fullerene needle-like crystal using the experimental setup in the present study, respectively. It was assumed that the C_{60}-C_{70} fullerene needle-like crystals were flexed before fracture as shown in Figs. 6(a)–(c), and the δ just before fracture was estimated to be 0.50 μm for the 1st crystal or 1.1 μm for the 2nd crystal using Figs. 6(d) and (e), respectively. When the E was supposed to be 80 GPa, as in the case for the C_{60}-C_{70} fullerene needle-like crystals with a diameter of more than 1000 nm [23], the maximum value of the σ_{ben}, that is the tensile strength, was calculated to be 71 MPa for the 1st crystal or 58 MPa for the 2nd crystal. These values are approximately six times larger than the tensile strength of the C_{60} fullerene needle-like crystals (11.5 MPa) calculated using the maximum buckling force of 230 nN and the diameter of 160 nm [17]. Therefore, we demonstrate that the C_{60}-C_{70} fullerene needle-like crystals have larger specific strength, which means the tensile strength per unit density, than that of alumina using the density of the C_{60}-C_{70} fullerene needle-like crystals of 1.7 g cm^{-3} and alumina of 3.95 g cm^{-3}.

According to Figs. 5 (b) and (c), the parameters a = 14 μm and W = 20 μm or a = 7.9 μm and W = 10 μm were obtained for the 1st or 2nd C_{60}-C_{70} fullerene needle-like crystal

using the experimental setup in the present study, respectively. When σ_{ben} = 58–71 MPa, the K was calculated to be 1.1–1.3 MPa $m^{\frac{1}{2}}$ using Eq. (1). Therefore, the fracture toughness of the C_{60}-C_{70} fullerene needle-like crystals is lower than that of alumina (1.5–1.9 MPa $m^{\frac{1}{2}}$) [32]. This means that the C_{60}-C_{70} fullerene needle-like crystals tend to undergo brittle fracture because of their porous structure. Therefore, the C_{60}-C_{70} fullerene needle-like crystals can be applied for materials of electrodes and anchors as brittle materials.

The magnified SEM images of the particle structures are depicted in Figs. 7(a) and (b). The particles are thought to be composed of the solvated C_{60} molecules. It has been reported that the C_{60} fullerene needle-like crystals with a diameter of less than 1 μm contain toluene with 1 wt% even after vacuum drying at room temperature for 120 min [33]. Therefore, it is possible that the C_{60}-C_{70} fullerene needle-like crystals in this work, which had a diameter of 20–40 μm, contain toluene with more than 1 wt%. The magnified SEM images of the fibrous surfaces are presented in Figs. 7(c) and (d). The fibrous surfaces have been reported to result from ductile fractures [26–27]. Thus, the fibrous surfaces are thought to occur when solvated fullerene molecules expanded and were subjected to strain in the present study. We can obtain ductile solvated C_{60}-C_{70} fullerene needle-like crystals which exhibit lower tensile strength and higher fracture toughness than the C_{60}-C_{70} fullerene needle-like crystals in order to apply them for strained materials such as electric feeder lines.

4. Conclusion

The C_{60}-C_{70} fullerene needle-like crystals were bent until the fracture and then observed using FIB-SEM, which exhibited a porous structure and brittleness caused by the stress concentration at pores. We demonstrate that the C_{60}-C_{70} fullerene needle-like crystals have the tensile strength of 58–71 MPa, which is approximately six times larger than that of the C_{60} fullerene needle-like crystals. This tensile strength makes the specific

strength of the C_{60}-C_{70} fullerene needle-like crystals larger than that of alumina. Moreover, the C_{60}-C_{70} fullerene needle-like crystals exhibit the fracture toughness of 1.1–1.3 MPa $m^{\frac{1}{2}}$, which is approximately one eighth of that of alumina. Therefore, the C_{60}-C_{70} fullerene needle-like crystals are useful for materials of electrodes and anchors as brittle materials.

The C_{60}-C_{70} fullerene needle-like crystals contain a small amount of solvent, which led to partial ductility. Thus, we can improve the fracture toughness of the C_{60}-C_{70} fullerene needle-like crystals and can change their plasticity from brittle to ductile by solvent in order to apply them for strained materials such as electric feeder lines.

Acknowledgments

This work was partly supported by the Center of Materials Research for Low Carbon Emission of National Institute for Materials Science and by the Japan Society for the Promotion of Science KAKENHI Grant No. 26600007.

References

[1] Kroto H W, Heath J R, O'Brien S C, et al. C_{60}: Buckminsterfullerene [J]. Nature, 1985, 318: 162-163.

[2] Krätschmer W, Lambt L D, Fostiropoulos K, Huffmant D R. Solid C_{60}: a new form of carbon [J]. Nature, 1990, 347: 354-358.

[3] Johnston H J, Hutchison G R, Christensen F M, et al. The Biological Mechanisms and Physicochemical Characteristics Responsible for Driving Fullerene Toxicity [J]. Toxicol. Sci., 2010, 114: 162-182.

[4] Goel A, Hebgen P, Sande J B V, et al. Combustion synthesis of fullerenes and fullerenic nanostructures [J]. Carbon, 2002, 40: 177-182.

[5] Miyazawa K (ed.). Fullerene Nanowhiskers [M]. Singapore: Pan Stanford Publishing Pte. Ltd., 2011.

[6] Miyazawa K. Synthesis and Properties of Fullerene Nanowhiskers and Fullerene Nanotubes [J]. J. Nanosci. Nanotechnol., 2009, 9: 41-50.

[7] Miyazawa K, Kuwasaki Y, Hamamoto K, et al. Structural characterization of C_{60} nanowhiskers formed by the liquid/liquid interfacial precipitation method [J]. Surf. Interface Anal., 2003, 35: 117-120.

[8] Larsson M P, Hansen J K, Lucyszyn S. DC Characterisation of C_{60} Whiskers and Nanowhiskers [J]. ECS Transactions, 2007, 2: 27-38.

[9] Xu M, Pathak Y, Fujita D, et al. Covered conduction of individual C_{60} nanowhiskers [J]. Nanotechnology, 2008, 19: 075712.

[10] Ji H X, Hu J S, Wan L J, et al. Controllable crystalline structure of fullerene nanorods and transport properties of an individual nanorod [J]. J. Mater. Chem., 2008, 18: 328-332.

[11] Ogawa K, Kato T, Ikegami A, et al. Electrical properties of field-effect transistors based on C_{60} nanowhiskers [J]. Appl. Phys. Lett., 2006, 88: 112109.

[12] Somani P R, Somani S P, Umeno M. Toward organic thick film solar cells: Three dimensional bulk heterojunction organic thick film solar cell using fullerene single crystal nanorods [J]. Appl. Phys. Lett., 2007, 91: 173503.

[13] Miyazawa K, Minato J, Zhou H, et al. Structure and electrical properties of heat-treated fullerene nanowhiskers as potential energy device materials [J]. J. Eur. Ceram. Soc., 2006, 26: 429-434.

[14] Sathish M, Miyazawa K, Sasaki T. Nanoporous Fullerene Nanowhiskers [J]. Chem. Mater., 2007, 19: 2398-2400.

[15] Shrestha L K, Sathish M, Hill J P, et al. Alcohol-induced decomposition of Olmstead's crystalline A_g(I)–fullerene heteronanostructure yields ‘bucky cubes’ [J]. J. Mater. Chem. C. 2013, 1: 1174-1181.

[16] Murayama H, Fullerene ryousan gijyutu. In: Densi Zairyou [M]. Kogyo Chosakai Publishing Co.,Ltd., Tokyo, 2003, 34‑37 (in Japanese).

[17] Asaka K, Kato R, Miyazawa K, et al. Buckling of C_{60} whiskers [J]. Appl. Phys. Lett., 2006, 89: 071912.

[18] Saito K, Miyazawa K, Kizuka T. Bending Process and Young's Modulus of Fullerene C_{60} Nanowhiskers [J]. Jpn. J. Appl. Phys., 2009, 48: 010217.

[19] Kizuka T, Miyazawa K, Tokumine T. Solvation-Assisted Young’s Modulus Control of Single-Crystal Fullerene C_{70} Nanowhiskers [J]. J. Nanotech., 2012, 12: 583817.

[20] Larsson M P, Lucyszyn S. Mechanical characterization of C_{60} whiskers by MEMS bend testing [J]. J. Phys.: Conf. Series, 2009, 159: 012006.

[21] Watanabe M, Miyazawa K, Kojima K, et al. Bending Deformation of C_{60} Nanowhiskers in Solution and Air [J]. IEEJ Trans SM, 2008, 128: 321-324.

[22] Konno T, Wakahara T, Miyazawa K. Synthesis and structural analysis of C_{60}–C_{70} two-component fullerene nanowhiskers [J]. J. Crystal Growth, 2015, 416: 41-46.

[23] Matsuura D, Konno T, Wakahara T, et al. Young's Modulus of C_{60}/C_{70} Alloy Nanowhiskers. 2014 Tsukuba Nanotechnology Symposium (TNS'14), Extended Abstracts, July, Tsukuba, 2014.

[24] Miyazawa K, Hirata C, Wakahara T. Influence of the solution volume on the growth of C_{60} nanowhiskers [J]. J. Cryst. Growth, 2014, 405: 68-72.

[25] Kato R, Miyazawa K. Cross-sectional structural analysis of C_{60} nanowhiskers by transmission electron microscopy [J]. Diam. Relat. Mater., 2011, 20: 299-303.

[26] Schulson E M, Barker D R. A brittle to ductile transition in NiAl of a critical grain size [J]. Scr. Metall., 1983, 17: 519-522.

[27] Peterlik H, Roschger P, Klaushofer K, et al. From brittle to ductile fracture of bone [J]. Nat. Mater., 2006, 5: 52-55.

[28] Murakami Y. Ouryokusyutyu no Kngaekata [M]. Yokendo, Tokyo, 2005.

[29] Oji K. Nakai Y., Zairyoukyoudo [M]. Corona Publishing Co. Ltd., Tokyo, 2010.

[30] Duckworth W H. Precise tensile properties of ceramic bodies [J]. J. Am. Ceram. Soc., 1951, 34: 1-9.

[31] The Engineer's book vo.18 [M]. HEISHIN Ltd., Kobe, 2012.

[32] Prielipp H, Knechtel M, Claussen N, et al. Strength and fracture toughness of aluminum/alumina composites with interpenetrating networks [J]. Mat. Sci. Eng. A-struct, 1995, 197: 19-30.

[33] Watanabe M, Hotta K, Miyazawa K, et al. GC-MS analysis of the solvents contained in C_{60} nanowhiskers [J]. J. Phys.: Conf. Series, 2009, 159: 012010.

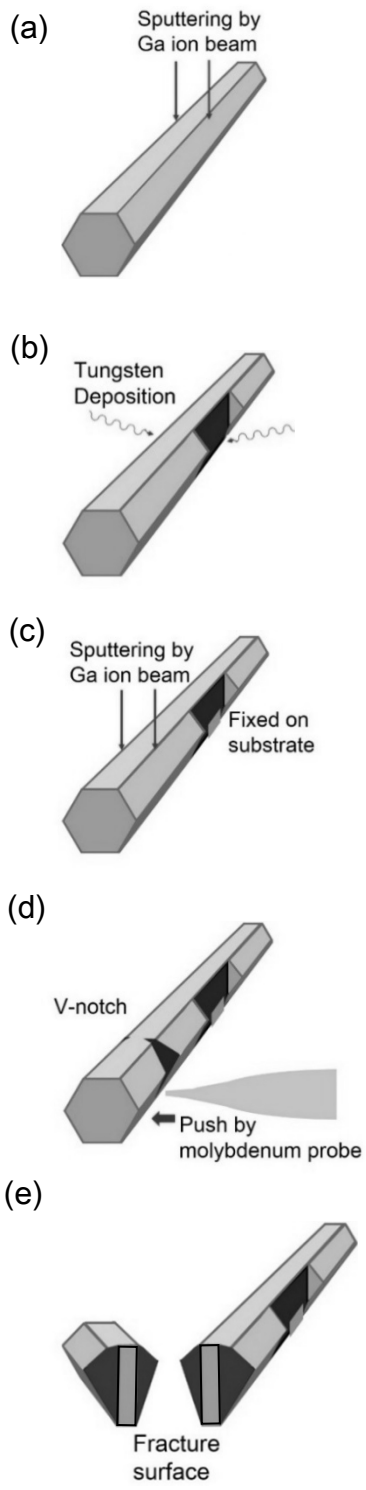

Fig. 1. Outline of the process to fracture a C_{60}-C_{70} fullerene needle-like crystal. (a) Side surface formation, (b) fixture to a substrate, (c) slit formation, (d) bending, and (e) fracture.

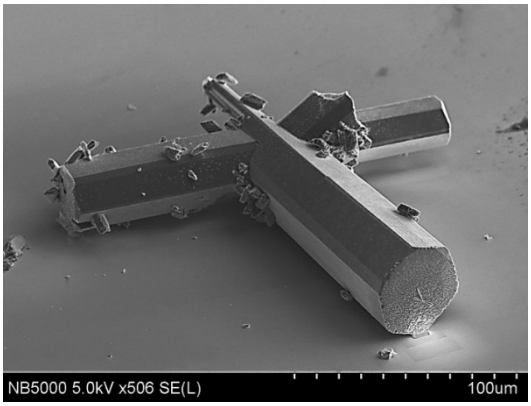

Fig. 2. The SEM image of a C_{60}-C_{70} fullerene needle-like crystal.

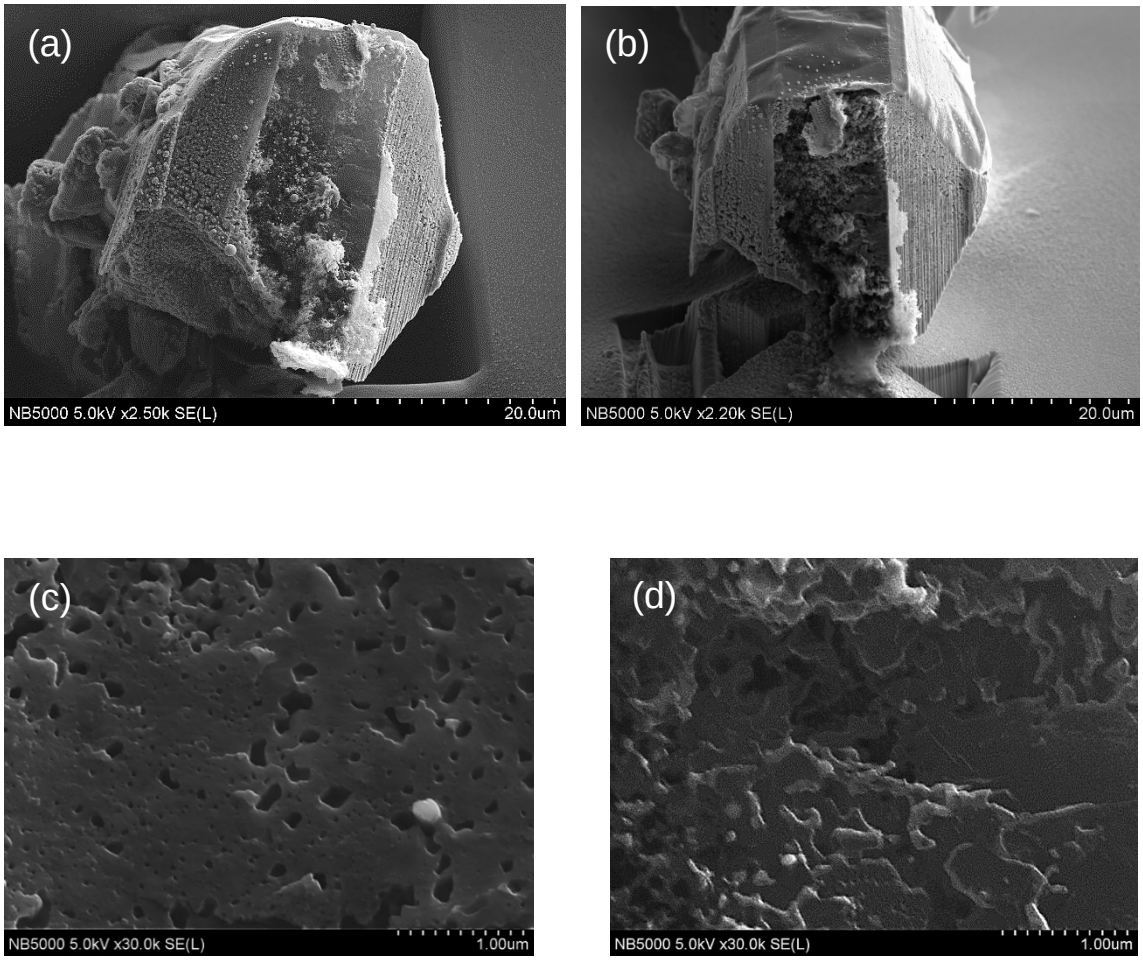

Fig. 3. (a),(b) The SEM images of the fracture surfaces of the C_{60}-C_{70} fullerene needle-like crystals. (c),(d) The SEM images of the smooth fracture surfaces of the C_{60}-C_{70} fullerene needle-like crystals.

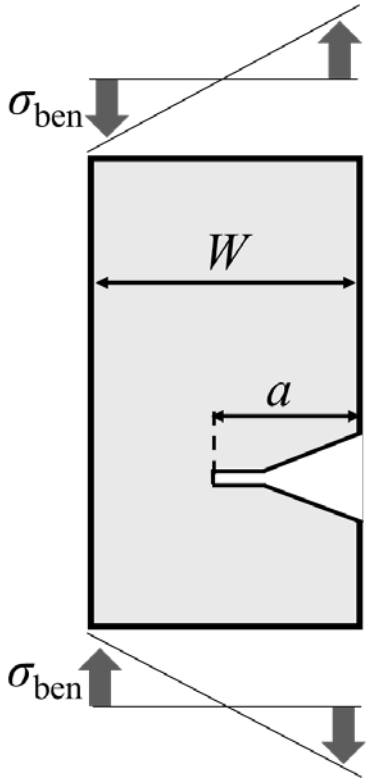

Fig. 4. Schematic of bending in this study. Here, a is the length of the crack on one side, W is the thickness of bending samples and σ_{ben} is the bending stress.

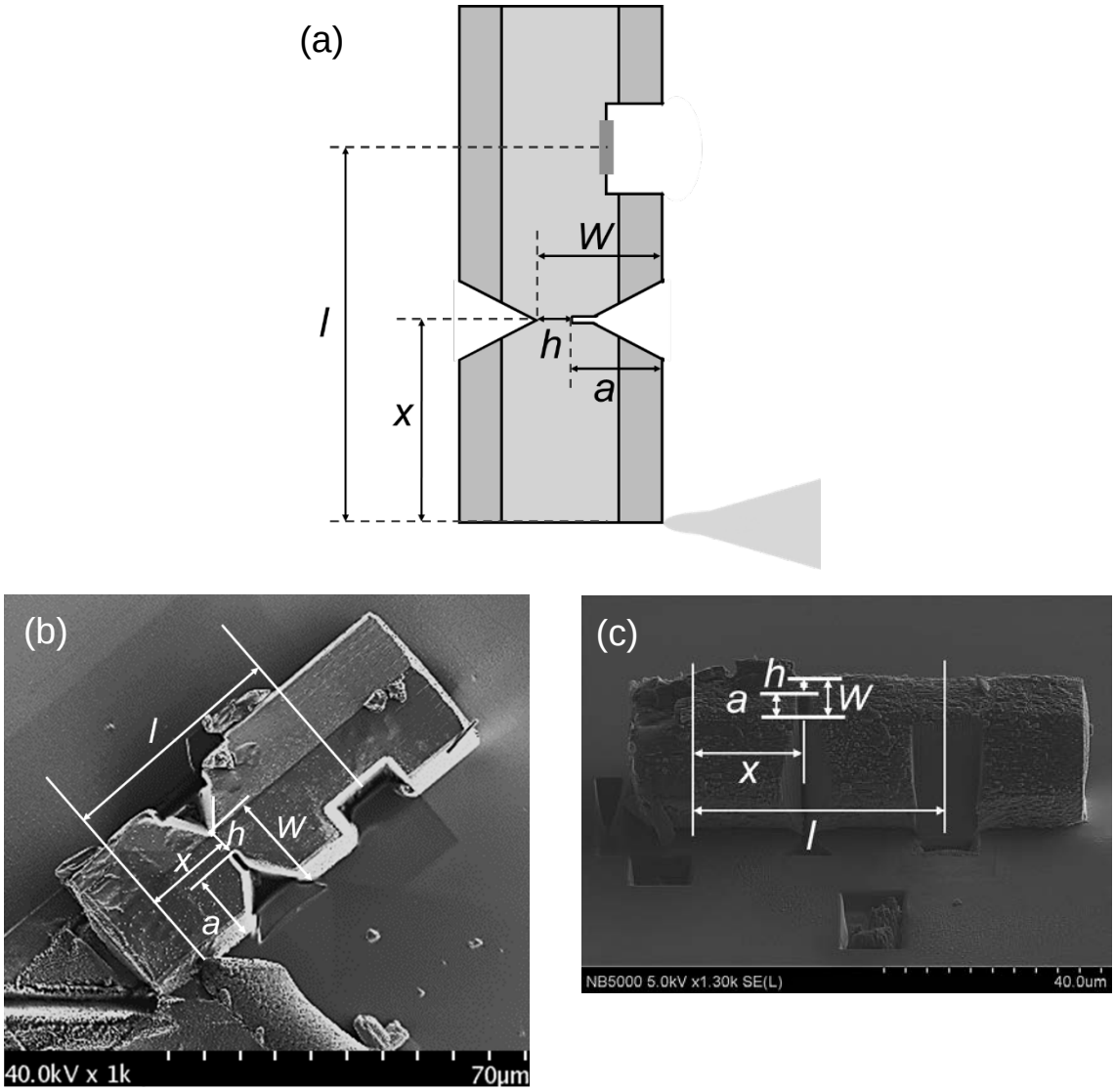

Fig. 5. (a) The definitions for the respective lengths. (b),(c) SEM images of C_{60}-C_{70} fullerene needle-like crystal with the respective lengths. Here, *l* is the distance between the points of effort and fulcrum, *h* is the length of the cross section parallel to the load, *x* is the distance between the points of the effort and the load, *a* is the length of crack on one side, and *W* is the thickness of bending samples.

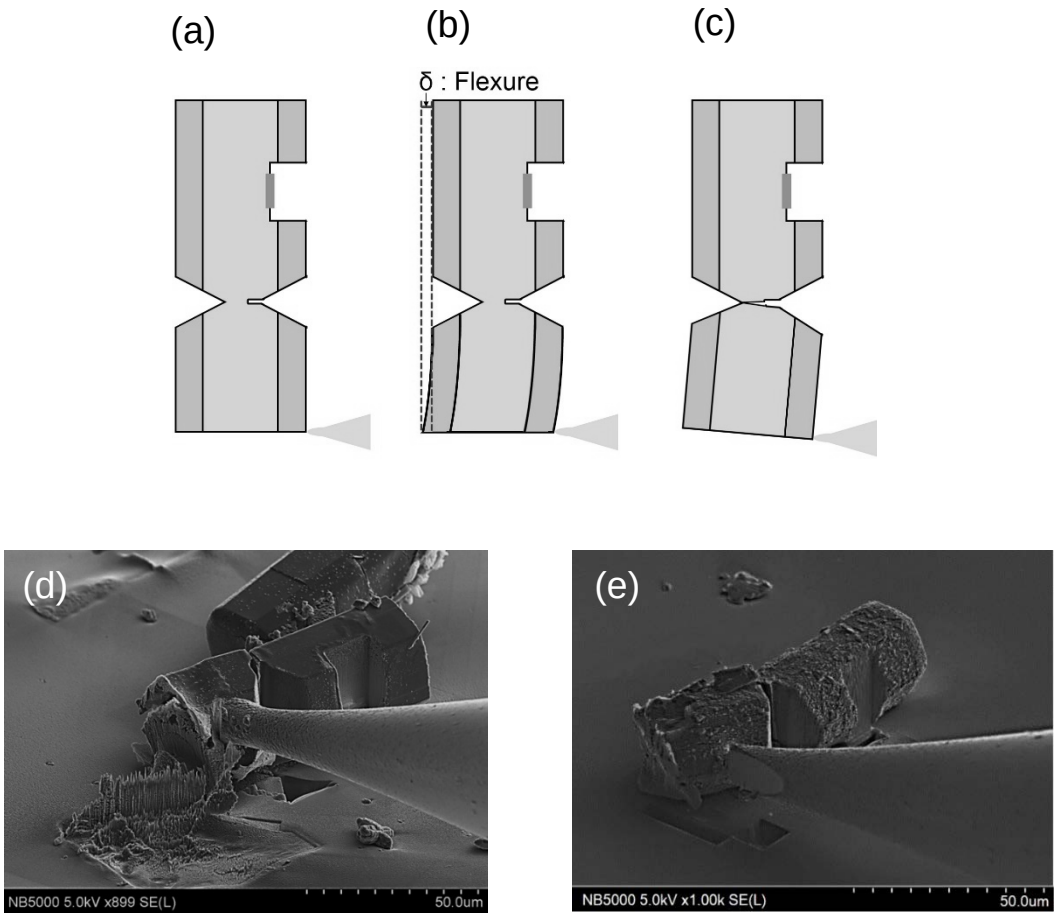

Fig. 6. Schematics of a C_{60}-C_{70} fullerene needle-like crystal (a) with no load, (b) just before fracture, and (c) just after fracture. (d),(e) The SEM images of C_{60}-C_{70} fullerene needle-like crystals just after fracture.

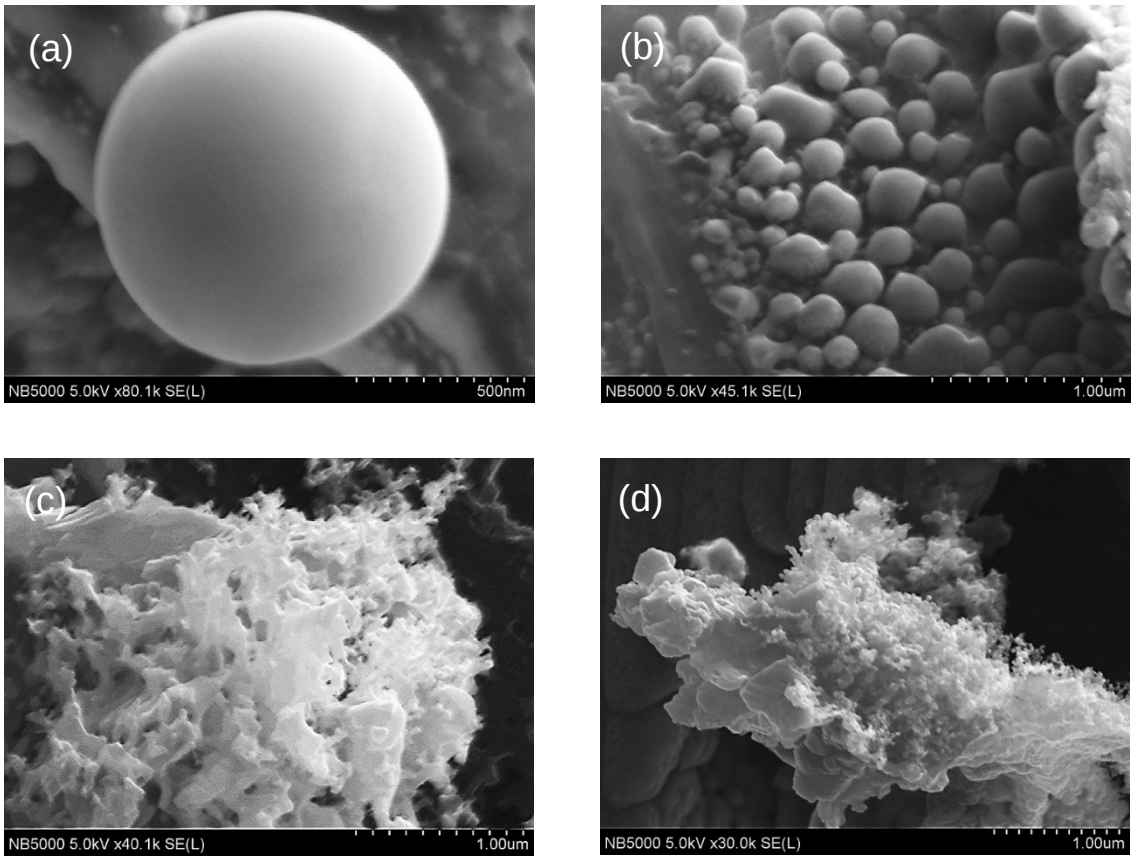

Fig. 7. (a),(b) The SEM images of the particle structures at the fracture surfaces of a C_{60}-C_{70} fullerene needle-like crystal. (c),(d) The SEM images of the fibrous structure at the fracture surfaces of a C_{60}-C_{70} fullerene needle-like crystal.